Renewable Energy 158 (2020) 23–31

Contents lists available at ScienceDirect

Renewable Energy

journal homepage: www.elsevier.com/locate/renene

Bioelectromethanogenesis reaction in a tubular Microbial Electrolysis Cell (MEC) for biogas upgrading

Marco Zeppilli *, Lorenzo Cristiani , Edoardo Dell'Armi , Mauro Majone

Department of Chemistry, University of Rome Sapienza, Piazzale Aldo Moro 5, 0015, Rome, Italy

ARTICLE INFO

Article history:
Received 12 December 2019
Received in revised form
5 May 2020
Accepted 22 May 2020
Available online 30 May 2020

Keywords:
Biogas upgrading
Microbial electrolysis cell
Bioelectrochemical systems
CO_2 removal
Bioelectromethanogenesis
Biofuels

ABSTRACT

The utilization of a pilot scale tubular Microbial Electrolysis Cell (MEC), has been tested as an innovative biogas upgrading technology. The bioelectromethanogenesis reaction permits the reduction of the CO_2 into CH_4 by using a biocathode as electrons donor, while the electroactive oxidation of organic matter in the bioanode partially sustains the energy demand of the process. The MEC has been tested with a synthetic wastewater and biogas by using two different polarization strategies, i.e. the three-electrode configuration, in which a reference electrode is utilized to set the potential at a chosen value, and a two-electrode configuration in which a fixed potential difference is applied between the anode and the cathode. The tubular MEC showed that the utilization of a simple two electrode configuration does not allow to control the electrodic reaction in the anodic chamber, which causes the increase of the energy consumption of the process. Indeed, the most promising performances regarding the COD and CO_2 removal have been obtained by controlling the anode potential at +0.2 V vs SHE with a three electrode configuration, with an energy consumption of 0.47 kWh/kgCOD and 0.33 kWh/Nm^3 of CO_2 removed, which is a comparable energy consumption with respect the available technologies on the market.

1. Introduction

A potential innovative route for the biological CO_2 methanization [1], i.e. the conversion of CO_2 into CH_4, involved the utilization of bioelectrochemical systems (BES) in which the microorganism's metabolism is controlled through an electrochemical device [2]. The microbial metabolism control is based on the electron exchange between a microorganism and an electrode by the extracellular electron transfer mechanism (EET) [3]. The electrochemical interface constituted by the electrode and the microorganisms can be named bioelectrode; If the electrodic material act as electron acceptor, the interface is called bioanode while in the case of an electrodic material working as electron donor, the interface is defined a biocathode [4]. Several environmental applications of BES are recently reported in the literature like the electricity production from wastewater [5], the removal of toxic and persistent contaminants in the groundwater [6], the nutrient recovery like ammonia [7], phosphorus and potassium, and the biological production of hydrogen [8], methane [9] and short chain volatyle fatty acids [10].

The bioelectromethanogenesis reaction involved the utilization of a biocathode in which the electroactive microorganisms are capable to reduce the CO_2 into CH_4 by using an electrode as electron donor [11]. The potential application of the bioelectromethanogenesis reaction for the energy storage of electrical power [12,13] under CH_4 is currently receiving attentions in several research groups with the development of the Bioelectrochemical power to gas concept (BPtG) [14]. In the BPtG concept, the bioelectrochemical production of CH_4 can be adopted for the utilization of the electricity surplus production from renewable resources (i.e. photovoltaic or wind electricity) [14,15]to reduce the CO_2 into CH_4, which can be easily stored and distributed with the existing natural gas power infrastructures and facilities [16]. In this context the biogas upgrading process [17], i.e. the removal of the CO_2 from the biogas produce by the anaerobic digestion, results an interesting application of the bioelectrochemical reduction of the CO_2 into CH_4 due to the high percentage of CO_2 in the biogas [18]. Several authors proposed the utilization of a MEC for the biogas upgrading into biomethane with different configuration including in-situ approaches, i.e. the direct insertion of polarized electrodes in the anaerobic digestion reactor [19–21], or an ex-situ approach in which a post treatment of the liquid and gaseous effluents of the digester are separately treated in the MEC [22–24]. Moreover,

* Corresponding author.
E-mail address: marco.zeppilli@uniroma1.it (M. Zeppilli).

https://doi.org/10.1016/j.renene.2020.05.122

Nomenclature

MEC	Microbial electrolysis cell
CE	Coulombic efficiency
CCE	Cathodic capture efficiency
SHE	Standard hydrogen electrode
AEM	Anion exchange membrane
VSS	Volatile suspended solids
VFA	Volatile fatty acids
COD	Chemical oxygen demand

along with the CO_2 reduction, another CO_2 removal mechanism have been recently identified in the CO_2 sorption as HCO_3^- ion caused by the alkalinity generation the biocathode [25], more in details, the alkalinity generation in the biocathode directly depends by the transport of ionic species different from protons and hydroxyls for the electroneutrality maintenance [26]. Even if the CO_2 sorption results the main CO_2 removal mechanisms, the CO_2 reduction into CH_4 along with the anodic reaction are necessary for the electrical current generation which in turn stimulate the ionic transport for the electroneutrality maintenance [27]. The CO_2 removal through the bioelectromethanogenesis reaction coupled with the anodic bioelectrochemical oxidation of the organic matter have been explored in bench scale reactors under several operating conditions including different substrates [28], different organic loading rates [29] and different anodic potentials [30]. Even if the bioelectromethanogenesis reaction is a well know at laboratory scale, with several configurations, no study has demonstrated that the respective designs can indeed be operated satisfactorily beyond the litre-scale, moreover, other pilot scale bioelectrochemical reactors, mainly devoted to bioelectricity production, have shown that construction and maintenance can be demanding especially when low conductivity solutions, such as real wastewater, are used for run the process [31].Here, in this study a first scale up system with a tubular geometry has been developed for the biogas upgrading through the bioelectromethanogenesis reaction coupled with the oxidation of COD in the anodic chamber. The utilization of the bioelectrochemical oxidation of the organic matter in the anodic chamber to sustain the cathodic bioelectromethanogenesis reaction is mainly related with the reduction of the energy consumption of the process due to the substantially lower potential required for the COD bioelectrochemical oxidation, which results around 0 V vs SHE [32] with respect the water oxidation, which required a potential of +1.23 V vs SHE, i.e. part of the required energy to run the process derived from the oxidation of the organic compounds in the anodic feeding solution. The tubular geometry of the MEC here proposed has been adopted to simulate a sorption column in which the alkalinity, bioelectrochemically generated by the reactions, enhance the CO_2 sorption without the use of any additional chemicals. Two different polarization strategies have been adopted for the operation of the tubular MEC, i.e. a three-electrode configuration, in which the anodic potential is controlled using a reference electrode and a potentiostat, and a two-electrode configuration in which the potential difference between anode and cathode is fixed by the potentiostat. The reason of the utilization of a two-electrode configuration resulted by the fact that usually industrial electrochemical processes are conducted under fixed potential or fixed current using a power supplier, a simpler device instead of a potentiostat able to work with a three-electrode configuration. The correspondent electrochemical analysis losses as well as the overpotential determination on the anodic and cathodic reactions have been also utilized to assess the different mechanisms involved in the anodic and cathodic chamber of the reactor.

2. Material and methods

2.1. Tubular MEC set up

The tubular MEC has been set-up using a plexiglass cylindric reactor of 12 L, where the inner anodic chamber (3.14 L) was separated from the external cathodic chamber (8.86 L) by a tubular anion exchange membrane (Fumasep FAD-PEEK, FumatechGmbH) (Fig. 1). Both concentric chambers (anodic and cathodic) were filled with graphite granules with a bed porosity of 0.57; the anodic and cathodic compartment were equipped with an external glass chamber for the liquid and the gas sample collection. The anodic chamber was inoculated by using 1 L of activated sludge (10.5 gVSS/L) coming from a full-scale wastewater treatment plant producing a bioanode capable of treating a wastewater. During the startup process the anodic potential was controlled at + 0.2 V vs. SHE to select the electroactive microorganisms able to use the electrode as electron acceptor. In the meantime, the cathodic chamber was inoculated with 1 L of an anaerobic sludge (7.3 gVSS/L) coming from a thermophilic anaerobic digester. By using a peristaltic pump, the inner anodic chamber was continuously fed with a synthetic mixture of organic substrates with a flow rate of 6 L/d, resulting in a hydraulic retention time (HRT) of 12.6 h. The synthetic mixture was composed by: peptone (0.41 g/L), yeast extract (0.5 g/L), sodium acetate (0.19 g/L), glucose (0.94 g/L), NH_4Cl (0.125 g/L), $MgCl_2$ $6H_2O$ (0.1 g/L), K_2HPO_4 (4 g/L), $CaCl_2$ $2H_2O$ (0.05 g/L), 10 mL/L of a trace metal solution, and 1 mL/L of a vitamin solution. The outer cathodic chamber was initially filled with a mineral medium composed by NH_4Cl (0.125 g/L), $MgCl_2$ $6H_2O$ (0.1 g/L), K_2HPO_4 (4 g/L), $CaCl_2$ $2H_2O$ (0.05 g/L); the cathode chamber didn't received any liquid feeding solution and it was continuously fed by a gas mixture composed of CO_2 at 30% and N_2 at 70% to simulate the CO_2 content of a biogas, utilized for the safety operation of the continuous flow process in a laboratory environment. A digital barometer was used to determine the operating pressures at which the gas samples were analysed. In the cathodic compartment, the liquid phase was continuously recirculated using a peristaltic pump. The water diffusion through the AEM required a daily refill of the cathodic chamber with mineral medium. The reactor operated at controlled laboratory temperature of 25 °C. First, a three electrodes configuration was adopted by using a AMEL model 549 potentiostat and a reference Ag/AgCl electrode (+0.2 V vs. SHE) placed in the anodic chamber, i.e. the anode was the working electrode while the cathode acted as counter electrode. Two additional multimeters (Aim-TTI 1604) were connected to the circuit to measure the flowing current and the potential difference between the two electrodes (ΔV). Then, during the two-electrode operation, a potential difference between the anode and the cathode was set by using the potentiostat as a simple voltage power supplier.

2.2. Analytical methods

The chemical oxygen demand (COD) in the anode influent and effluent streams were assessed by using commercial COD cell test (Merck, Darmstadt, Germany). The methane content of the gas phase was analysed by sampling 50 μL of the headspace by a gas-tight Hamilton syringe and injecting it into a Varian 3400 gas-chromatograph (Lake Forest, CA, USA) (GC; 2 m × 2 mm glass column packed with 60/80 mesh Carbopack B/1% SP-1000; He carrier gas at 18 mL/min; oven temperature at 50 °C; FID temperature 260 °C).

The CO_2 determination was performed by injecting 50 μL of gaseous sample into a Dani Master gaschromatograph (stainless-

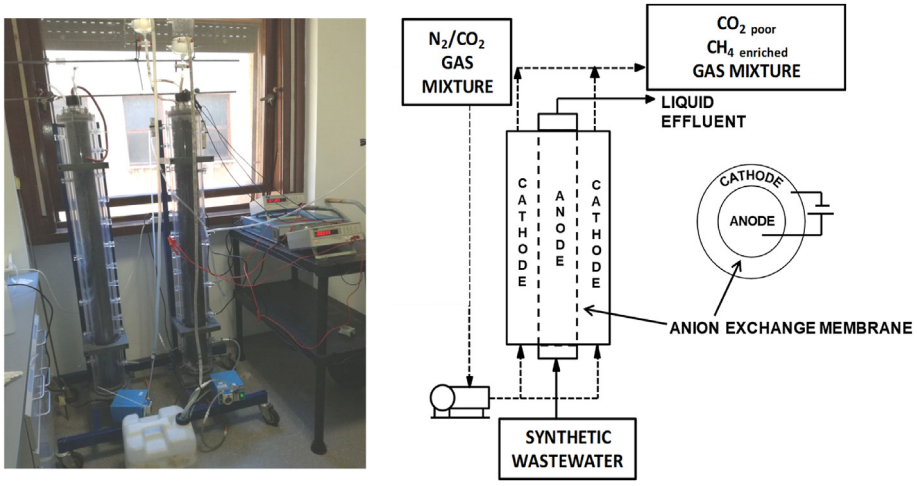

Fig. 1. Photography and schematic representation of the tubular MEC.

steel column packed with molecular sieve; He as carrier gas 18 mL/min; oven temperature 70 °C; thermal-conductivity detector (TCD) temperature 200 °C). The inorganic carbon was measured by TOC (Total Organic Carbon Analyzer)-V CSN (Shimadzu) on filtered samples (0.2 μm).

2.3. Calculations

The daily COD removal in the anodic chamber was assessed as the difference between the daily amount of influent and effluent COD (mg/d), according to the following equation (1):

$$COD_{removed}\left(\frac{mg}{d}\right) = F_{in}{*}COD_{in} - F_{out}{*}COD_{out} \quad (1)$$

in which COD_{in} (mg/L) and COD_{out} (mg/L) represent respectively the anodic influent and effluent COD while F_{in}(L/d) and F_{out} (L/d) are the influent and effluent flow rates in the anodic chamber (L/d). The COD removal efficiency can be also evaluated by:

$$COD_{removal\ efficiency\ (\%)} = \frac{F_{in}{*}COD_{in} - F_{out}{*}COD_{out}}{F_{in}{*}COD_{in}}{*}100 \quad (2)$$

The COD oxidation reaction can be expressed with the following general equation:

$$C_xH_yO_zN + (2x - z)H_2O \rightarrow xCO_2 + [y + (2x - z)]\,[e^- + H^+] + NH_3 \quad (3)$$

According to the water oxidation reaction, the daily amount of COD diverted into current was also expressed as equivalents of electrons

$$2H_2O \rightarrow O_2 + 4e^- + 4H^+ \quad (4)$$

The meq_{COD} was calculated from $mgCOD_{removed}$ by using a conversion factor of 4 meq/32 mgCOD.

The Coulombic Efficiency (CE%) represents the amount of oxidized COD directly converted into current; it was calculated as the ratio between the cumulative electric charge transferred in one day at the electrodes (meqi) and the cumulative equivalents released by the COD oxidation (meqCOD):

$$CE\ (\%) = \frac{meq_i}{meq_{COD}}{*}100 \quad (5)$$

The cumulative electric charge (meqi) was calculated by integrating the current (A) over time and dividing by the Faraday's constant (F = 96485 C/eq).

The methane production rate $rCH_{4(mmol)}$ (mmol/d) was also expressed in terms of equivalents $rCH_{4(eq)}$ (meq/d), considering the conversion factor of 8 meq/$mmol_{CH4}$, which derives from the following semi-reaction:

$$CO_2 + 8e^- + 8H^+ \rightarrow CH_4 + 2H_2O \quad (6)$$

$$rCH_{4(mmol)} * 8 = rCH_{4(meq)} \quad (7)$$

About the Cathode Capture Efficiency (CCE, %) which represent the efficiency of the bioelectromethanogenesis reaction, i.e. the amount of CO_2 reduced into CH_4 by the methanogenic consortium which use the electric current as reducing power source. The CCE was calculated by the ratio between the cumulative equivalents of produced methane (meq_{CH4}) and the cumulative equivalents of current (i.e. the charge):

$$CCE(\%) = \frac{meq_{CH4}}{meq_i}{*}100 \quad (8)$$

The energy efficiency (ηE) of the process, which is expressed by the ratio between the energy recovered from the methane production and the electrical energy utilized for the polarization of the process.

$$\eta E(\%) = \frac{n_{CH4} \times \Delta G_{CH4}}{\Delta V \times C}{*}100 \quad (9)$$

with ΔGCH_4 (−817.97 kJ/mol) and nCH_4 (mmol) representing the molar Gibbs free energy for methane combustion and the amount of produced methane, whereas ΔV represent the cell voltage between the cathode and anode and C the cumulative charge (Coulombs), calculated by integrating the current over time.

2.4. Inorganic carbon mass balance

The CO_2 daily removal (ΔCO_2, mmol/d) by each cathodic chamber has been evaluated by the following equation (10):

$$\Delta CO_2 = Qcat_{in}{*}CO_{2\ in} - Qcat_{out}{*}CO_{2\ out} \quad (10)$$

in which Q_{cat}in (L/d) and Q_{cat}out (L/d) are the influent and effluent

gas flow rates, respectively whereas CO_{2in} and CO_{2out} (mmol/L) represent the CO_2 concentrations in the influent and effluent gaseous cathodic streams respectively.

Since different forms of inorganic carbon (i.e. CO_2 and HCO_3^- ion) were present, the methane production and the CO_2 sorption (as HCO_3^- ion in the cathodic liquid phases) were both representing the main cathodic CO_2 removal mechanisms. The HCO_3^- ion in the cathodic chamber is removed by the migration of HCO_3^- ion from the cathodic chamber to the anodic one across the AEM membrane.

The following expression (11) represents the overall inorganic mass balance in the reactor:

$$Qcat_{in}*CO_{2\ in} + F_{in}*HCO_{3in}^- + F_{refill}*HCO_{3MM}^- = Qcat_{out}*(CO_{2\ out}) + r_{CH4(mmol)} + F_{out}*HCO_{3out}^- \quad (11)$$

where Q (L/d) are and F (L/d) are the volumetric flow rates of the gaseous and the liquid streams, respectively while CO_2 and HCO_3^- indicate the molar concentrations in gaseous and liquid phases expressed as inorganic carbon. Q_{cat}in is the influent gaseous flow rate in the cathodic chamber while Q_{cat}out is the outlet flow rate from the cathodic chamber; F_{in} and F_{out} are the anodic influent and effluent flow rates, F_{refill} is the refill flow rate of the cathodic chamber and $HCO_{3\,MM}^-$ is the concertation of bicarbonate in the mineral medium. The term $rCH_{4(mmol)}$ (mmol/d) represents the rate of the overall methane production.

The estimation of the contribution of the HCO_3^- to the ionic transport from the AEM cathode to the anode, is calculated from the overall inorganic mass balance by using the following expression (12):

$$HCO_{3(transf)}^- = F_{out}*HCO_{3out}^- - F_{in}*HCO_{3in}^- \quad (12)$$

then, it is possible to convert the molar daily amount of HCO_3^- transferred (13) in terms of current by

$$HCO_3^-\ (mA) = HCO_3^-\ (\text{transf})\text{AEM}*n*\frac{F}{86400} \quad (13)$$

where n is the charge of the bicarbonate ion, F is the Faraday constant and 86400 represents the seconds in a day.

2.5. Electrochemical losses

According to previous experiments [32] the equilibrium potential of the anodic and cathodic electrodic reactions have been assessed applying the Nernst equation to the acetate oxidation and hydrogen evolution. The equilibrium potentials for the anodic ($Ean_{(eq)}$) and cathodic ($Ecath_{(eq)}$) reactions were calculated according to the Nernst equation by considering the standard potentials and the average concentrations evaluated for each potentiostatic condition. Due to the capability of electroactive microorganisms to convert mainly short chain VFA produce by fermentative microorganisms, acetate oxidation semi-reaction can be used as model anodic reaction (14). Thus, the Nernst equation for the anodic reaction resulted (15):

$$2HCO_3^- + 8\,e^- + 9H^+ \rightarrow CH_3COO^- - + 2H_2O \quad (14)$$

$$E_{an\ (eq)} = E^0 + \frac{RT}{8F}\ln\frac{[HCO_3^-]^2*[H^+]^9}{[CH_3COO^-]} \quad (15)$$

E^0 was 0.187 V and acetate, HCO_3^- and H^+ concentrations were the average values in the anodic effluent during the considered steady state period (the acetate concentration was assumed equal to the COD concentration in the anodic effluent).

For the reduction reaction (16), the proton reduction was chosen because, the average cathodic potential (17) resulted more negative than the equilibrium potential ($E^{0'} = -0.41$ V vs SHE at pH = 7) in all explored conditions. The proton concentration was calculated from the average pH in the cathodic chamber for the considered period, while the hydrogen partial pressure was taken of 0.0001 atm [33], which represents the lower limit for hydrogenophilic methanogens activity and was chosen because, no hydrogen was detected in the cathodic chamber during all over the MEC operation.

$$2H^+ + 2\,e^- \rightarrow + H_2 \quad (16)$$

$$E_{cath\ (eq)} = E^0 + \frac{RT}{2F}\ln\frac{[H^+]^2}{[pH_2]} \quad (17)$$

The formal potentials of each chamber were measured by a multimeter with respect to the respective reference electrode and were named $Ean_{(formal)}$ and $Ecath_{(formal)}$ for the anode and cathode chamber, respectively. According to the literature [34], the difference between the formal potential and the equilibrium potential expressed the overpotentials for the anodic (η_{an}) (12) and cathodic (η_{cath}) (16) reactions according to the following equations (18) and (19):

$$\eta_{an} = E_{an(formal)} - E_{an(eq)} \quad (18)$$

$$\eta_{cath} = E_{cath(formal)} - E_{cath(eq)} \quad (19)$$

in which,

The experimental cell voltage (ΔV_{exp}) which represents the voltage drop between anode and cathode electrodes was determined by a multimeter. Moreover, the cell voltage of an electrolysis cell can be expressed as (20) follows:

$$\Delta V = E_{cath(meas)} - E_{an(meas)} + \sum\eta \quad (20)$$

where $\sum\eta$ represents the sum of the overpotentials that cause an additional energy loss in the system. The $\sum\eta$ is referred to the energy losses due to the migration and the convection of the ions for the electroneutrality maintenance and it depends by several parameters such as ionic conductivity and the fluid dynamic behavior. In the whole electrochemical characterization, a formal cell voltage has been calculated by the formal anodic and cathodic potential measured by the multimeter, thus, by calculated the difference between the experimental (21) and the formal cell voltage (22), the overall voltage drop of the cell was assessed for each potentiostatic condition.

$$\Delta V_{(formal)} = E_{cath(formal)} - E_{an(formal)} \quad (21)$$

$$\sum\eta = \Delta V_{(exp)} - \Delta V_{(formal)} \quad (22)$$

2.6. COD mass balance

The COD mass balance was utilized in order to describe and characterize the different COD removal mechanisms involved in the anodic and cathodic chamber. Three different mechanisms of COD removal have been considered in the different potentiostatic condition, i.e. the overall methane production at the cathode chamber, the biomass production evaluated by the daily volatile suspended solids (VSS) coming out from the anodic chamber and the average current converted as the daily oxygen production. The latter

mechanism was considered only during the two electrode potentiostatic condition and it was evaluated according to the following expression:

$$COD_{O2}\left(\frac{mgCOD}{d}\right) = \frac{i\,(mA)*86400\frac{s}{d}*32\ g/mol}{96485\frac{C}{eq}*4\frac{eq}{mol}} \quad (23)$$

In which I represent the average current, 86400 are the seconds in a day and the 96485 C/eq is the Faraday's constant, used to convert the charge into equivalents; 4 are the equivalents released by water oxidation and 32 is the conversion factor to convert the moles of oxygen into grams of COD.

The COD mass recovery was calculated the following expression-:

$$COD_{recovery}\,(\%) = \frac{COD_{CH4} + COD_{VSS} + COD_{O2}}{COD_{removed}}*100 \quad (24)$$

3. Results and discussions

3.1. Start-up and +0.2 V vs SHE MEC operation

After the inoculation of the anodic and cathodic chamber of the tubular MEC, a start-up period characterized by the polarization of the anodic chamber at +0.2 V vs SHE with a three-electrode configuration has been adopted to stimulate the anodic biofilm growth on the graphite granules. During the start-up period, the synthetic organic mixture was continuously recirculated in the anodic chamber under batch mode. The start-up period that showed the capability of the anodic chamber to oxidize the organic matter by using the electrodic material as electron acceptor, then the anode chamber operation was shifted to a continuous flow mode with an average flow rate of 6 L/d, that corresponds to an HRT of 0.52 days. The continuous flow mode with the anodic chamber poised at +0.2 V vs SHE was maintained for 20 days (i.e. 38 HRT) to characterize a steady state condition of the reactor with the three-electrode configuration. An average COD removal of 4850 ± 85 mgCOD/d was obtained (Fig. 2), corresponding to a COD removal efficiency of 56 ± 7%. Considering the removed COD and the current output of the tubular MEC (Fig. 3), that resulted on average 86 ± 5 mA, the coulombic efficiency during the +0.2 V vs SHE run, was only 13 ± 4%. The main reduction product produced in the cathodic chamber of the tubular MEC was the methane, which was produced with an average rate of 300 ± 48 meq/d; the corresponding coulombic efficiency of the cathodic reaction, also named cathode capture efficiency (CCE), resulted on average 390 ± 8%, which indicated the presence of an additional mechanism of methane production. This additional mechanism was likely an acetoclastic activity of the cathodic biofilm as suggested from the presence of a stable COD concentration of 500 mgCOD/L in the cathodic chamber of the MEC (Fig. 2). By considering the methane overproduction due to acetoclastic activity, a daily diffusion of 1800 mgCOD/d from the anode to the cathode chamber was determined. The COD migration from the anode to the cathode resulted in a loss of efficiency of the bioelectrochemical reactions introducing a COD shortcut inside the reactor.

3.2. Two electrode configuration at different applied voltages

After the characterization of the +0.2 V vs SHE run, with a three electrode configuration, in order to perform a more conventional potentiostatic control of the electrochemical process with a simpler apparatus, the potentiostatic control of the tubular MEC was

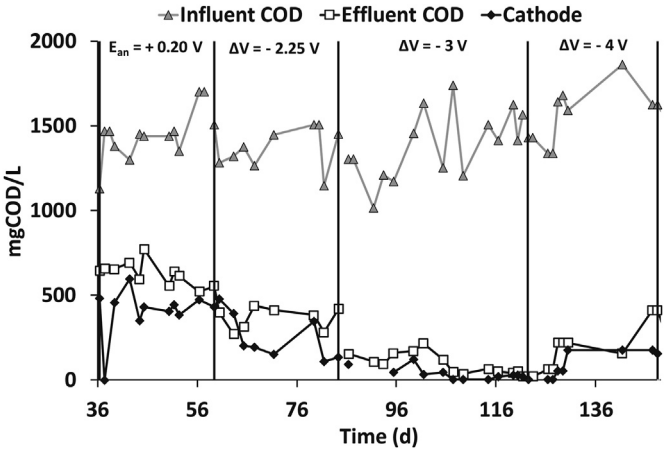

Fig. 2. COD time profile of the different reactor streams during all the potentiostatic conditions explored.

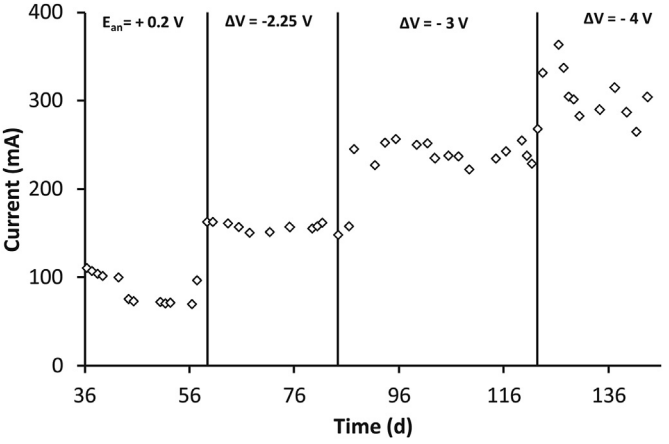

Fig. 3. Current time profile during all the potentiostatic conditions explored.

changed to a two-electrode configuration in which the potential difference between the anode and the cathode is fixed to the desired value. The potential difference has been set to −2.25 V and maintained for 24 days (46 HRT); the average current raised up to the value of 154 ± 9 mA (Fig. 3); along with the increase of the current, the removed COD in the anode chamber (Fig. 2) and the methane production in the cathodic chamber (Fig. 4) increased up to the average value of 5982 ± 60 mgCOD/d and 449 ± 32 meq/d, respectively. Those values permitted the assessment of an average CE of and a CCE of 18 ± 8% and 325 ± 14% for the potentiostatic condition at −2.25 V. In order to increase the reaction rates in the anodic and cathodic chamber the potential difference was further increase to −3.00 and −4.00 V, maintaining the potentiostatic condition at least for 20 days (i.e. HRT higher than 38); the average current obtained at −3.00 and −4.00 V resulted 237 ± 14 and 282 ± 39 mA, respectively.

While the COD removal in the anodic chamber showed an increase with the increase of the potential difference, with average values of 7631 ± 55 and 8360 ± 105 mgCOD/d corresponding in a removal efficiency of 92 ± 8 and 90 ± 5% of the COD, the methane production decreased as the potential difference increased (and consequent the current increased), to average values of 367 ± 13 and 261 ± 18 meq/d (Fig. 4).

During the latter two potentiostatic condition, the coulombic efficiency of the anodic chamber reached slightly higher values

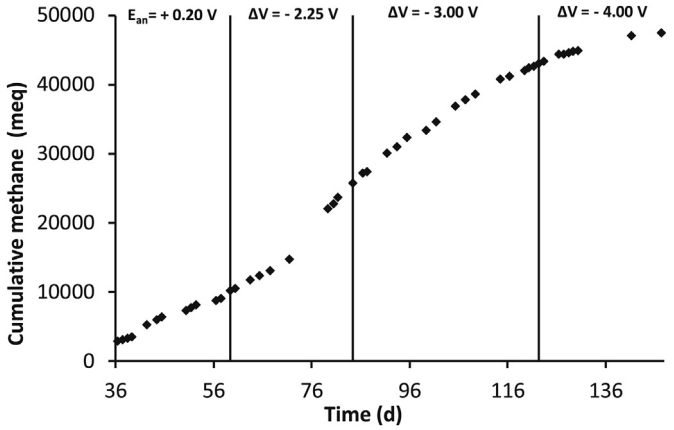

Fig. 4. Cumulative cathodic methane production during the different potentiostatic conditions explored.

corresponding to 22 ± 5 and 24 ± 6% low values, while the cathode capture efficiency (CCE) decreased from the value of 173 ± 5 for the −3.00 V condition to 103 ± 9% for the −4.00 V condition. The cathodic methane production was probably influenced by the dynamic of the microbial population, in which the acetogenic methanogens converted the organic substrates coming from the anodic chamber into methane. The coulombic efficiency of both anodic and cathodic reactions resulted strongly influenced by the COD shortcut from the anodic and cathodic chamber, where this shortcut decreased as the ΔV increased.

All the main bioelectrochemical parameters obtained in the different potentiostatic conditions are summarized in Table 1.

3.3. Electrochemical losses characterization

The formal potentials of the anodic ($E_{an(formal)}$) and cathodic ($E_{cath(formal)}$) chambers, along with the experimental cell voltage ($\Delta V_{(exp)}$) were utilized for the determination of the reaction overpotentials, linked to the electrodic reactions, and for the determination of the overall potential drop due to the ohmic resistance of the electrolyte and to presence of the anion exchange membrane. The reaction overpotentials in the anodic and cathodic chamber have been calculated by considering the difference between the formal and the thermodynamic potential ($E_{an(eq)}$ and $E_{cath(eql)}$) evaluated by using the Nernst equation. Because the different values of the anodic formal potential obtained in each condition, the anodic reaction overpotential need to be assessed by considering the proper oxidation reaction, i.e. for the +0.2 V vs SHE, in which the anodic potential is controlled by a three electrode configuration, the COD oxidation resulted the electrodic reaction to be considered with a E_{eq} of −0.65 V vs SHE, on the contrary, in the −3.00 and −4.00 V condition, the anodic formal resulted +1.36 and + 1.83 V vs SHE which suggests that the water oxidation reaction, with a E_{eq} of +0.76 V vs SHE, occurred in the anodic chamber. Moreover, in the −2.25 V condition, in which an anodic formal potential of +0.66 V vs SHE was recorded, as reported in the literature [35] the average potential of COD oxidation and oxygen evolution can be reasonable utilized to describe the anodic electrodic condition, which resulted −0.06 V vs SHE. As a consequence, as reported in Table 2, the anodic overpotentials evaluated in the different potentiostatic conditions for the anodic reaction resulted in the range of 0.6–1.07 V, the latter evidence indicates that the electrochemical behaviour of the polarized cell tends to the reaction overpotentials minimization by shifting the oxidation reaction through the less energy demanding process. Regarding the cathodic reaction, the reaction overpotential was driven by the proton reduction which proceed with similar potential values in the different potentiostatic conditions adopted, the formal potential of the cathodic reaction remained in the range of −0.8 to −1.2 V vs SHE, while the $E_{cath(eq)}$ resulted on average −0.32 V vs SHE in every potentiostatic condition (Table 2). The relation of the anodic and cathodic reaction overpotentials with the average current in the different potentiostatic condition, Fig. 5-A, showed the slightly dependence of the reaction overpotentials with the average current which means that the electrodic overpotentials are mainly driven by mass transfer of the reactants and the activation energy of the reaction on the electrodic material. On the contrary, as Fig. 5-B shows, the voltage drop observed between the experimental cell voltage ($\Delta V_{(exp)}$) and the formal cell voltage ($\Delta V_{(formal)}$) strongly depends by the average current flowed in the cell, as expected, the voltage drop between the two terms increased by the increase of the current which clearly indicates the predominance of energy losses linked to the ohmic resistance of the cell [36].

3.4. COD mass balance

The COD mass balance of the explored potentiostatic conditions was assessed in order to describe the main mechanisms involved in COD removal. The detectable COD removal mechanisms resulted the methane production in the cathodic chamber, both by electrochemical and acetoclastic mechanisms, and the VSS outcoming daily with the anodic effluent. By this approach in the COD mass balance, the lost COD, i.e. the COD removed did not justified by methane production or biomass growth, resulted in a high

Table 2
Main results about the electrochemical losses characterization.

Potentiostatic Condition	+0.2 V vs SHE	- 2.25	- 3.00	- 4.00
$E_{anode(eq)}$	−0.65	−0.06	+0.76	+0.76
$E_{cathode\ (eq)}$	−0.30	−0.32	−0.32	−0.33
$E_{anode\ (formal)}$	+0.20	+0.66	+1.36	+1.83
$E_{cathode\ (formal)}$	- 0.8	- 1.1	−1.1	−1.2
$\eta_{\ anode}$ (V)	0.85	0.6	0.6	1.07
$\eta_{\ cathode}$ (V)	−0.50	−0.78	−0.78	−0.87
$\Delta V_{(exp)}$ (V)	−1.10	−2.25	−3.00	−4.00
$\Delta V_{(formal)}$ (V)	−1.0	−1.76	−2.46	−3.03
$\Sigma\eta$ (V)	0.1	0.49	0.54	0.97

Table 1
Main bioelectrochemical parameters obtained during the explored potentiostatic conditions.

Potentiostatic Condition	+0.2	- 2.25	- 3.00	- 4.00
Current (mA)	86 ± 5	154 ± 9	237 ± 14	282 ± 39
COD removed (mgCOD/d)	4850 ± 85	5982 ± 60	7631 ± 55	8360 ± 105
COD removal efficiency (%)	56 ± 7	72 ± 13	92 ± 8	90 ± 5
Coulombic Efficiency (CE, %)	13 ± 4	18 ± 8	22 ± 5	24 ± 6
Methane production (meq/d)	300 ± 48	449 ± 32	367 ± 13	261 ± 18
Cathode Capture Efficiency (CCE, %)	390 ± 8	325 ± 14	173 ± 5	103 ± 9

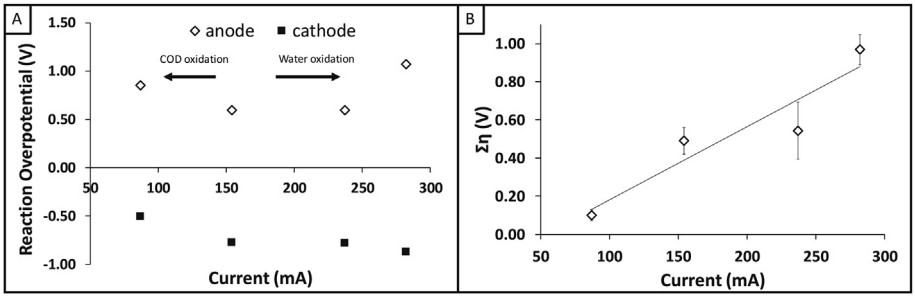

Fig. 5. Reaction overpotentials (A) and overall potential drop (B) with respect the average current flowing in the different potentiostatic conditions.

percentage which resulted much more relevant in the −3.00 and −4.00 V potentiostatic conditions. According to the previous described effect of the anodic potential increase during the two-electrode configuration; according to the electrochemical data (i.e. the formal potential of the anodic reaction) during the −2.25 V, −3.00 and −4.00 V potentiostatic condition, the oxygen evolution was estimated by the average current flowing in the cell. The oxygen evolution is supported by the average anodic formal potential observed during the two electrodes condition, i.e. oxygen can support the aerobic oxidation of the COD into CO_2 which cannot be directly accounted in the COD mass balance. For the two electrodes condition, −2.25, −3.00 and −4.00 V, the oxygen production terms increased considerably the amount of recovered COD of the mass balance. As shows in Table 3, the mass balance for the −3.00 and −4.00 V potentiostatic condition resulted in a mass recovery of 71 ± 3 and 61 ± 6%, in this case hypothesis linked to the underestimation of the biomass growth in the anodic chamber and the possibility to have some abiotic COD oxidation by the evolution of hydrogen peroxide, can affect the mass balance recovery.

3.5. CO_2 mass balance and bicarbonate transport

During all the potentiostatic conditions explored, the CO_2 removal in the cathodic chamber showed similar values with average values in the range of 300 mmol/d. As before mentioned, two CO_2 removal mechanisms, i.e. the methane production and the CO_2 sorption as HCO_3^- ion, occurred in the MEC cathodic chamber. The amount of CO_2 effectively converted into CH_4, as reported in Table 4, resulted in a percentage between the 10 and the 19% of the overall CO_2 removed from the cathode, even if the percentage of CO_2 converted in CH_4 is overestimated due to COD migration between anode and cathode, the percentage resulted comparable to the literature [27]. Throughout all of the conditions explored, the HCO_3^- profile in the different reactor streams (Fig. 6) shows a higher HCO_3^- concentration in the cathodic chamber of the tubular MEC with respect the anodic HCO_3^- concentration, moreover, the HCO_3^- concentration in the anodic effluent, resulted higher than the concentration in the influent HCO_3^-, indicating a net transport of HCO_3^- from the cathode to the anode chamber. The HCO_3^- transport from the cathode to the anode chamber can be attributed to two different mechanisms, the diffusion of the bicarbonate due to the concentration gradient between anode and cathode chamber, and the migration of the HCO_3^- for the electroneutrality maintenance from the cathode to the anode due to the presence of an AEM membrane. Considering the difference of HCO_3^- concentration between the influent and the effluent of the anodic chamber, the flux of bicarbonate transported across the AEM membrane has been determined in all the potentiostatic conditions explored. Even if, is not possible to distinguish the two different mechanisms, due to the similar HCO_3^- transport values obtained in the different conditions, the hypothesis of the predominance of a diffusion mechanism resulted by the evidence of a drop down of the HCO_3^- contribution to the ionic current transport (around 36 mmol/d in all

Table 4
CO_2 removal CH_4 production and HCO_3^- transport obtained during the different potentiostatic conditions.

Potentiostatic Condition	+0.2	- 2.25	- 3.00	- 4.00
CO_2 removal (mmol/d)	303 ± 12	292 ± 19	299 ± 9	321 ± 22
rCH_4 (mmol/d)	38 ± 6	56 ± 4	46 ± 3	33 ± 2
$HCO_{3\,transf}^-$ (mmol/d)	30 ± 6	33 ± 2	43 ± 4	38 ± 1

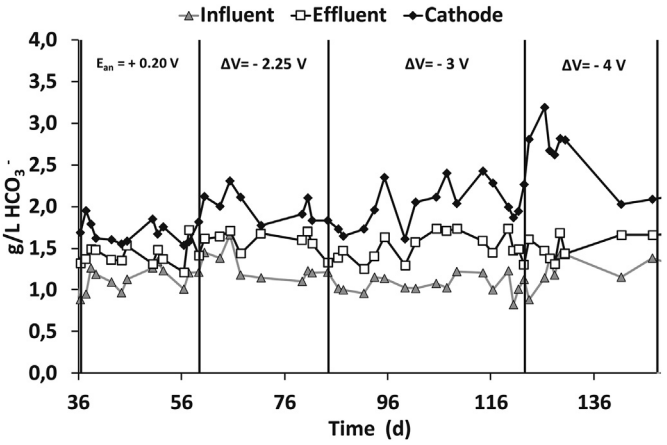

Fig. 6. Bicarbonate time course in the different reactor streams during all the potentiostatic conditions explored.

Table 3
COD mass balance in the different potentiostatic conditions explored.

Potentiostatic Condition	+0.2 V vs SHE	- 2.25	- 3.00	- 4.00
COD removed (mgCOD/d)	4850 ± 85	5982 ± 60	7631 ± 55	8360 ± 105
COD CH_4 (mgCOD/d))	2400 ± 384	3592 ± 256	2936 ± 104	2088 ± 144
COD VSS (mgCOD/d)	869 ± 64	1517 ± 55	818 ± 29	963 ± 48
COD O_2 (mgCOD/d)	–	1103 ± 55	1698 ± 55	2020 ± 279
COD recovery (%)	67 ± 10	101 ± 7	71 ± 3	61 ± 6

the condition) from 46 ± 9% to 16 ± 4% of the overall current flowing in the circuit in the different potentiostatic conditions.

3.6. Energy evaluation of the process

The energy consumed by the tubular MEC was assessed by measuring the applied voltage and the average current flowing in the circuit; the kWh consumed per day were utilized for the assessment of the energetic cost of each single operation, i.e. the COD removal in the anodic chamber and the CO_2 removal by the external cathodic chamber. Concerning the COD removal, the run at +0.2 V vs SHE (e.g. three electrode configuration) showed the lowest and energy consumption) with average values of 0.47 kWh/kgCOD removed and 0.33 and kWh/Nm^3 of CO_2 removed, respectively, these values are comparable with the two benchmark technologies (i.e. activated sludge for the COD removal and Water scrubbing for the CO_2 removal). By increasing the potential applied to the MEC at −2.25 -3.00 and −4.00 V (Fig. 7), it has been obtained only a significant increase of the energy consumption of the process rather than an increase in the COD and CO_2 removal from the MEC. The energy efficiency of the process, which represent the ratio between the energy recovered by the methane production and the electrical energy utilized to polarize the cell, resulted strongly affected by the overestimation of the methane produced in the first two potentiostatic conditions. The methane overproduction, caused by the COD migration from the anode to the cathode, resulted in energy efficiencies higher than 100% in the first two potentiostatic condition in which the energy efficiencies of the process resulted 399 ± 24 and 220 ± 19%, respectively. The resulting energy efficiencies are not consistent with the experimental results of the process because indicates a net energy production of the process instead of an energy consumption. Finally, during the −3.00 and −4.00 V (two electrode configuration condition), the energy efficiency resulted 74 ± 6 and 19 ± 5% which better describes the energy recover obtained by the cathodic methane production.

4. Conclusions

The results showed the feasibility of the process with the tubular geometry that permitted the anodic oxidation of substrates coupled with the CO_2 reduction into CH_4. However, with respect previous experiments performed in a flat bench scale reactor [27], a consistent loss of efficiency in terms of conversion of organic matter oxidation into current (i.e. the coulombic efficiency) has been obtained. On other hand, the cathodic performances, particularly the CO_2 removal, resulted highly increased by the tubular geometry with an average CO_2 removal of 300 mmol/d corresponding to the removal of 13.2 gCO_2/d, during the different potentiostatic conditions explored. The most promising application of the tubular MEC resulted the CO_2 removal also for the low energy consumption of 0.33 kWh/Nm^3 CO_2 removed obtained during the three-electrode configuration at +0.2 V vs SHE. The three-electrode configuration with the anode potential controlled at +0.2 V vs SHE showed the better energetic performance with energy consumptions for the COD removal and CO_2 removal of 0.47 kWh/kgCOD and 0.33 kWh/Nm^3 that resulted lower values with respect the energy consumption of the commercially available technologies on the market which result 1.2 kWh/kgCOD [37] for the activated sludge process and 0.8 kWh/Nm^3 CO_2 for the Water Scrubbing technology [38]. Finally, the main effect of the shift in the polarization strategy of the tubular MEC resulted in the loss of the anodic potential control, i.e. without a three electrodes configuration, the anodic oxidation evolved through the water oxidation with the main effect of increasing of the energy loss on the electrodic reaction.

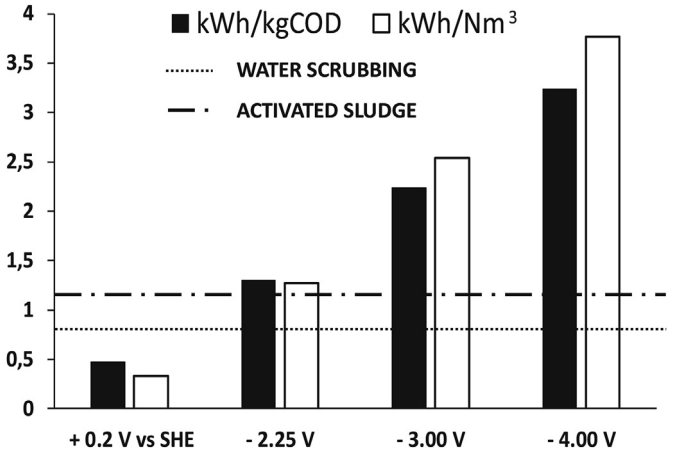

Fig. 7. Energy consumption for COD and CO_2 removal obtained during the different potentiostatic conditions and comparison with the selected benchmark technologies.

Funding

"This project has received funding from the European Union's Horizon 2020 research and innovation programme under grant agreement No 688338 (NoAw project)".

Declaration of competing interest

The authors declare that they have no known competing financial interests or personal relationships that could have appeared to influence the work reported in this paper.

CRediT authorship contribution statement

Marco Zeppilli: Investigation, Validation, Writing - original draft, Writing - review & editing. **Lorenzo Cristiani:** Investigation, Validation, Writing - original draft. **Edoardo Dell'Armi:** Investigation. **Mauro Majone:** Supervision, Writing - review & editing, Funding acquisition.

Acknowledgements

Giuliano Fazi is acknowledged for his skilful assistance during the experimental activity.

Appendix A. Supplementary data

Supplementary data to this article can be found online at https://doi.org/10.1016/j.renene.2020.05.122.

References

[1] K. Müller, M. Fleige, F. Rachow, D. Schmeißer, Sabatier based CO2-methanation of flue gas emitted by conventional power plants, Energy Proc. 40 (2013) 240–248, https://doi.org/10.1016/j.egypro.2013.08.028.
[2] B.E. Logan, B. Hamelers, R. Rozendal, U. Schroder, J. Keller, S. Freguia, P. Aelterman, W. Verstraete, K. Rabaey, Microbial fuel cells: methodology and technology, Environ. Sci. Technol. 40 (17) (2006) 5181–5192.
[3] S. Freguia, K. Rabaey, Z. Yuan, J. Keller, Syntrophic processes drive the conversion of glucose in microbial fuel cell anodes, Environ. Sci. Technol. 42 (21) (2008) 7937–7943.
[4] M. Rosenbaum, F. Aulenta, M. Villano, L.T. Angenent, Cathodes as electron donors for microbial metabolism: which extracellular electron transfer mechanisms are involved? Bioresour. Technol. 102 (1) (2011) 324–333.
[5] D. Pant, G. Van Bogaert, L. Diels, K. Vanbroekhoven, A review of the substrates used in microbial fuel cells (MFCs) for sustainable energy production,

Bioresour. Technol. 101 (6) (2010) 1533–1543, https://doi.org/10.1016/j.biortech.2009.10.017.
[6] P. Ledezma, J. Jermakka, J. Keller, S. Freguia, Recovering nitrogen as a solid without chemical dosing: bio-electroconcentration for recovery of nutrients from urine, Environ. Sci. Technol. Lett. 4 (3) (2017) 119–124.
[7] F. Aulenta, R. Verdini, M. Zeppilli, G. Zanaroli, F. Fava, S. Rossetti, M. Majone, Electrochemical stimulation of microbial cis-dichloroethene (cis-DCE) oxidation by an ethene-assimilating culture, N. Biotech. 30 (6) (2013) 749–755.
[8] B.E. Logan, D. Call, S. Cheng, H.V.M. Hamelers, T.H.J.A. Sleutels, A.W. Jeremiasse, R.A. Rozendal, Microbial electrolysis cells for high yield hydrogen gas production from organic matter, Environ. Sci. Technol. 42 (23) (2008) 8630–8640, https://doi.org/10.1021/es801553z.
[9] M. Villano, G. Monaco, F. Aulenta, M. Majone, Electrochemically assisted methane production in a biofilm reactor, J. Power Sources 196 (22) (2011) 9467–9472, https://doi.org/10.1016/j.jpowsour.2011.07.016.
[10] I. Vassilev, F. Kracke, S. Freguia, J. Keller, J.O. Krömer, P. Ledezma, B. Virdis, Microbial electrosynthesis system with dual biocathode arrangement for simultaneous acetogenesis, solventogenesis and carbon chain elongation, Chem. Commun. 55 (30) (2019) 4351–4354.
[11] M. Villano, F. Aulenta, A. Giuliano, C. Ciucci, T. Ferri, M. Majone, Bioelectrochemical reduction of CO2 to CH4 via direct and indirect extracellular electron transfer by a hydrogenophilic methanogenic culture, Bioresour. Technol. 101 (2010) 3085–3090.
[12] Z. Huang, L. Lu, D. Jiang, D. Xing, Z.J. Ren, Electrochemical hythane production for renewable energy storage and biogas upgrading, Appl. Energy 187 (2017) 595–600, https://doi.org/10.1016/j.apenergy.2016.11.099.
[13] N. Scarlat, J.-F. Dallemand, F. Fahl, Biogas: developments and perspectives in europe, Renew. Energy 129 (2018) 457–472.
[14] F. Geppert, D. Liu, M. van Eerten-Jansen, E. Weidner, C. Buisman, A. ter Heijne, Bioelectrochemical power-to-gas: state of the art and future perspectives, Trends Biotechnol. 34 (11) (2016) 879–894, https://doi.org/10.1016/j.tibtech.2016.08.010.
[15] M. Child, C. Kemfert, D. Bogdanov, C. Breyer, Flexible electricity generation, grid exchange and storage for the transition to a 100% renewable energy system in Europe, Renew. Energy 139 (2019) 80–101.
[16] M. Götz, J. Lefebvre, F. Mörs, A. McDaniel Koch, F. Graf, S. Bajohr, R. Reimert, T. Kolb, Renewable Power-to-Gas: a technological and economic review, Renew. Energy 85 (2016) 1371–1390.
[17] E. Ryckebosch, M. Drouillon, H. Vervaeren, Techniques for transformation of biogas to biomethane, Biomass Bioenergy 35 (5) (2011) 1633–1645, https://doi.org/10.1016/j.biombioe.2011.02.033.
[18] S. Cheng, D. Xing, D.F. Call, B.E. Logan, Direct biological conversion of electrical current into methane by electromethanogenesis, Environ. Sci. Technol. 43 (10) (2009) 3953–3958.
[19] I. Angelidaki, L. Treu, P. Tsapekos, G. Luo, S. Campanaro, H. Wenzel, P.G. Kougias, Biogas upgrading and utilization: current status and perspectives, Biotechnol. Adv. 36 (2) (2018) 452–466, https://doi.org/10.1016/j.biotechadv.2018.01.011.
[20] Z. Dou, C.M. Dykstra, S.G. Pavlostathis, Bioelectrochemically assisted anaerobic digestion system for biogas upgrading and enhanced methane production, Sci. Total Environ. 633 (2018) 1012–1021, https://doi.org/10.1016/j.scitotenv.2018.03.255.
[21] M. Cerrillo, M. Viñas, A. Bonmatí, Anaerobic digestion and electromethanogenic microbial electrolysis cell integrated system: increased stability and recovery of ammonia and methane, Renew. Energy 120 (2018) 178–189.
[22] P. Batlle-Vilanova, S. Puig, R. Gonzalez-Olmos, A. Vilajeliu-Pons, M.D. Balaguer, J. Colprim, Deciphering the electron transfer mechanisms for biogas upgrading to biomethane within a mixed culture biocathode, RSC Adv. 5 (64) (2015) 52243–52251, https://doi.org/10.1039/c5ra09039c.
[23] A. Kokkoli, Y. Zhang, I. Angelidaki, Microbial electrochemical separation of CO2 for biogas upgrading, Bioresour. Technol. 247 (Supplement C) (2018) 380–386, https://doi.org/10.1016/j.biortech.2017.09.097.
[24] M. Zeppilli, M. Simoni, P. Paiano, M. Majone, Two-side cathode microbial electrolysis cell for nutrients recovery and biogas upgrading, Chem. Eng. J. 370 (2019) 466–476, https://doi.org/10.1016/j.cej.2019.03.119.
[25] H. Xu, K. Wang, D.E. Holmes, Bioelectrochemical removal of carbon dioxide (CO2): an innovative method for biogas upgrading, Bioresour. Technol. 173 (2014) 392–398, https://doi.org/10.1016/j.biortech.2014.09.127, 0.
[26] T.H.J.A. Sleutels, H.V.M. Hamelers, R.A. Rozendal, C.J.N. Buisman, Ion transport resistance in Microbial Electrolysis Cells with anion and cation exchange membranes, Int. J. Hydrogen Energy 34 (9) (2009) 3612–3620, https://doi.org/10.1016/j.ijhydene.2009.03.004.
[27] M. Zeppilli, A. Lai, M. Villano, M. Majone, Anion vs cation exchange membrane strongly affect mechanisms and yield of CO2 fixation in a microbial electrolysis cell, Chem. Eng. J. 304 (2016) 10–19, https://doi.org/10.1016/j.cej.2016.06.020.
[28] M. Zeppilli, D. Pavesi, M. Gottardo, F. Micolucci, M. Villano, M. Majone, Using effluents from two-phase anaerobic digestion to feed a methane-producing microbial electrolysis, Chem. Eng. J. 328 (2017) 428–433, https://doi.org/10.1016/j.cej.2017.07.057.
[29] M. Villano, S. Scardala, F. Aulenta, M. Majone, Carbon and nitrogen removal and enhanced methane production in a microbial electrolysis cell, Bioresour. Technol. 130 (2013) 366–371.
[30] M. Villano, C. Ralo, M. Zeppilli, F. Aulenta, M. Majone, Influence of the set anode potential on the performance and internal energy losses of a methane-producing microbial electrolysis cell, Bioelectrochemistry 107 (2016) 1–6, https://doi.org/10.1016/j.bioelechem.2015.07.008.
[31] K. Rabaey, L. Angenent, U. Schröder, J. Keller, Bioelectrochemical systems: from extracellular electron transfer to biotechnological application, IWA Publishing 2009.
[32] M. Zeppilli, P. Paiano, M. Villano, M. Majone, Anodic vs cathodic potentiostatic control of a methane producing microbial electrolysis cell aimed at biogas upgrading, Biochem. Eng. J. 152 (2019) 107393.
[33] M. Villano, C. Ralo, M. Zeppilli, F. Aulenta, M. Majone, Influence of the set anode potential on the performance and internal energy losses of a methane-producing microbial electrolysis cell, Bioelectrochemistry 107 (2016) 1–6.
[34] T.H.J.A. Sleutels, H.V.M. Hamelers, R.A. Rozendal, C.J.N. Buisman, Ion transport resistance in Microbial Electrolysis Cells with anion and cation exchange membranes, Int. J. Hydrogen Energy 34 (9) (2009) 3612–3620.
[35] F. Harnisch, S. Wirth, U. Schröder, Effects of substrate and metabolite crossover on the cathodic oxygen reduction reaction in microbial fuel cells: platinum vs. iron(II) phthalocyanine based electrodes, Electrochem. Commun. 11 (11) (2009) 2253–2256.
[36] A. Bard, J. Faulkner, Electrochemical Methods Fundamentals and Applications, Wiley2001.
[37] P.L. McCarty, J. Bae, J. Kim, Domestic wastewater treatment as a net energy producer-can this be achieved? Environ. Sci. Technol. 45 (2011) 7100–7106.
[38] J.d. Hullu, J. Waassen, P. Van Meel, S. Shazad, J. Vaessen, Comparing Different Biogas Upgrading Techniques, vol. 56, Eindhoven University of Technology, 2008.